

Isospin-violating dark-matter-nucleon scattering via two-Higgs-doublet-model portals

Aleksandra Drozd,^a Bohdan Grzadkowski,^b John F. Gunion,^c Yun Jiang^{c,d,1}

^aTheoretical Particle Physics and Cosmology Group,
Physics Department, King's College London, London WC2R 2LS, UK

^bFaculty of Physics, University of Warsaw, Pasteura 5, 02-093 Warsaw, Poland

^cDepartment of Physics, University of California, Davis, CA 95616, U.S.A.

^dNBIA and Discovery Center, Niels Bohr Institute, University of Copenhagen,
Blegdamsvej 17, DK-2100, Copenhagen, Denmark

E-mail: Bohdan.Grzadkowski@fuw.edu.pl, gunion@physics.ucdavis.edu,
yunjiang@nbi.ku.dk

Abstract. We show that in a multi-Higgs model in which one Higgs fits the LHC 125 GeV state, one or more of the other Higgs bosons can mediate DM-nucleon interactions with maximal DM isospin violation being possible for appropriate Higgs-quark couplings, independent of the nature of DM. We then consider the explicit example of a Type II two-Higgs-doublet model, identifying the h or H as the 125 GeV state while the H or h , respectively, mediates DM-nucleon interactions. Finally, we show that if a stable scalar, S , is added then it can be a viable light DM candidate with correct relic density while obeying all direct and indirect detection limits.

Keywords: dark matter, two-Higgs-doublet model

¹Corresponding author.

Contents

1	Introduction	1
2	Direct detection of Dark Matter and isospin-violation	2
3	The 2HDMS Dark-Matter Model	4
3.1	Collider bounds from direct searches for Higgs bosons	6
3.2	Collider bounds from jet plus missing energy final states	7
3.3	Dark matter direct detection	8
3.4	Dark matter indirect detection	9
4	Conclusions	11

1 Introduction

One of most outstanding failures of the Standard Model (SM) is the lack of a candidate for dark matter (DM), the latter constituting 27% of the energy of the universe [1]. Many models have been proposed for DM in a variety of beyond-the-SM theories. Higgs bosons could play an important role in two ways. First, one or more Higgs could mediate interactions between nucleons and DM. Second, DM could itself be a Higgs boson. In this letter, we consider a two-Higgs-doublet model (2HDM) within which there are two CP-even Higgs bosons, h and H ($m_h < m_H$), where one fits the SM-like state at 125 GeV. We show that if the h and H mediate the interactions of DM with quarks we can arrange for the DM-nucleon interactions to be isospin-violating, thereby allowing light dark matter to be consistent with the LUX (2016) limits [2] at low DM mass, independent of the nature of the DM particle itself. Next, we demonstrate that if the 2HDM is extended to include a stable singlet scalar boson, S , whose interactions with quarks are mediated by the h and H , we can choose parameters so that the S can provide the observed relic density even for $m_S < 60$ GeV without violating any theoretical or phenomenological constraints.

The minimal SM extension (called xSM) for which DM might be a Higgs boson is to add a scalar singlet field S protected by a \mathbb{Z}'_2 symmetry under $S \rightarrow -S$, communicating with the SM via a $\lambda S^2 H^\dagger H$ interaction [3, 4]. However, to achieve correct relic DM abundance, $\Omega_S h^2$, for $m_S \lesssim 60$ GeV a rather large value of the portal coupling λ is required. This leads to both too large $\text{BR}(H_{\text{SM}} \rightarrow SS)$ and a direct DM detection cross section exceeding the old LUX (2013) upper limit [5].

Both problems can be cured in the 2HDMS model [6] in which a real gauge-singlet scalar, S , is added to the two doublet fields of the 2HDM. As above, if a \mathbb{Z}'_2 symmetry is imposed and we require that S not have a vacuum expectation value (vev) then the h and H of the 2HDM will be mass eigenstates and the S can be dark matter. The main idea is that if the h (H) is identified as the 125 GeV state (the h_{125} and H_{125} scenarios, respectively) it can have a very small portal coupling to S (and therefore

small SS branching ratio) while correct relic abundance can be achieved via relatively strong interactions of the H (h) with the S .

In addition to being able to achieve correct $\Omega_S h^2$ for a light S with small SS branching ratio of the SM-like Higgs, in the 2HDMS model with Type II Yukawa couplings one can avoid the LUX (2016) exclusion bounds for low mass DM. The key point is that in Type II models the couplings of the non-SM-like Higgs to up- and down-type quarks, and therefore to protons and neutrons are not the same, and, for appropriate parameter choices, can even have opposite sign leading to a very suppressed cross section for DM scattering off of a nucleus [5–9].

The paper is organized as follows. In Sec. II we briefly describe the current status of direct detection experiments and show how isospin-violating interactions of DM are possible in the Type II 2HDM context, independently of whether or not dark matter is a Higgs boson. In Sec. III we introduce the Type II 2HDMS and find parameters for which the S is a fully viable dark matter candidate. We end with a summary of our results.

2 Direct detection of Dark Matter and isospin-violation

DM is a compelling window to new physics and a primary means for its direct detection is via scattering off nucleons. Experimental results are typically translated into the event rate (or limit) for the spin-independent cross section for DM scattering off a nucleon $\sigma_{\text{DM}-N}^{\text{SI}}$ as a function of DM mass. The strongest exclusion limits are currently those from LUX [10] and, in the very-low mass regime (*i.e.* DM mass below 15 GeV), SuperCDMS [11].

Translating from experimental data to $\sigma_{\text{DM}-N}^{\text{SI}}$ involves many assumptions, including use of the Standard Halo Model (as in [10]) and elastic scattering at zero-momentum transfer with a short range contact interaction. In particular, limits on $\sigma_{\text{DM}-N}^{\text{SI}}$ are typically given assuming that DM couples equally to the neutron and proton, the strengths of these couplings being denoted by f_n and f_p — see [6] for details using our conventions. If $f_n/f_p \neq 1$, one must apply a rescaling factor Θ_X to convert the predicted DM-proton cross-section $\sigma_{\text{DM}-p}^{\text{SI}}$ to the DM-nucleon cross section $\sigma_{\text{DM}-N}^{\text{SI}}$ obtained assuming $f_n/f_p = 1$:

$$\sigma_{\text{DM}-N}^{\text{SI}} = \sigma_{\text{DM}-p}^{\text{SI}} \Theta_X(f_n, f_p), \quad (2.1)$$

where the rescaling factor Θ_X for a multiple isotope detector is defined in [6]. When $f_n/f_p \neq 1$, $\Theta_X(f_n, f_p)$ will depend upon the isotope abundances (which are detector-dependent) and can be as small as $\sim 10^{-4}$ when f_n/f_p is close to -1 , -0.8 , -0.7 for target nucleons Si, Ge, and Xe, respectively, (with weak dependence on m_S) [12].

As we now describe, such f_n/f_p values can be achieved in multi-Higgs models, independently of the nature of DM. One Higgs must be identified with the SM-like state at 125 GeV and have very weak coupling to DM, while one or more of the other Higgs bosons should be primarily responsible for mediating DM-quark interactions. As derived in [6], the general expression for f_n/f_p is

$$\frac{f_n}{f_p} = \frac{m_n F_u^n \tilde{\lambda}_U + F_d^n \tilde{\lambda}_D}{m_p F_u^p \tilde{\lambda}_U + F_d^p \tilde{\lambda}_D} \quad (2.2)$$

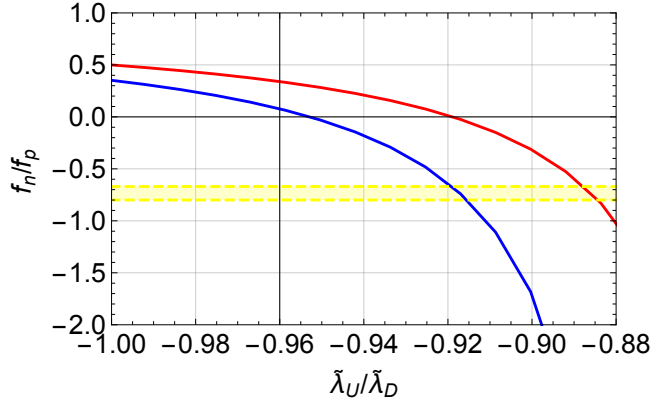


Figure 1. The correlation between f_n/f_p and $\tilde{\lambda}_U/\tilde{\lambda}_D$ with (red) and without (blue) QCD NLO corrections and using $f_{Tu}^n = 0.011$, $f_{Td}^n = 0.0273$, $f_{Ts}^n = 0.0447$ and $f_{Tu}^p = 0.0153$, $f_{Td}^p = 0.0191$, $f_{Ts}^p = 0.0447$, all as employed in micrOMEGAs [14]. The yellow band corresponds to f_n/f_p in the range -0.67 to -0.8.

where

$$F_u^N = f_{Tu}^N + \sum_{q=c,t} \frac{2}{27} f_{Tq}^N \left(1 + \frac{35}{36\pi} \alpha_S(m_q) \right) \quad (2.3)$$

$$F_d^N = f_{Td}^N + f_{Ts}^N + \frac{2}{27} f_{Tq}^N \left(1 + \frac{35}{36\pi} \alpha_S(m_b) \right) \quad (2.4)$$

($N = p, n$) and the scale-dependent α_S terms account for the QCD NLO corrections (not included in [6]) while $f_{Tq}^N = 1 - \sum_{q=u,d,s} f_{Tq}^N$. $\tilde{\lambda}_U$ and $\tilde{\lambda}_D$ are defined as follows

$$\tilde{\lambda}_U = \sum_{\mathcal{H}} \frac{\Lambda_{\mathcal{H}}}{m_{\mathcal{H}}^2} C_U^{\mathcal{H}}, \quad \tilde{\lambda}_D = \sum_{\mathcal{H}} \frac{\Lambda_{\mathcal{H}}}{m_{\mathcal{H}}^2} C_D^{\mathcal{H}}, \quad (2.5)$$

where $\sum_{\mathcal{H}}$ sums over the Higgs mediators contributing to the t -channel diagrams, $C_{U,D}^{\mathcal{H}}$ denote the \mathcal{H} couplings to up-, down-type quarks, respectively, normalized to their SM values, while the $\Lambda_{\mathcal{H}}$ are dimensionless parameters specifying the strengths of the \mathcal{H} couplings to a pair of DM particles. Fig. 1 shows the ratio f_n/f_p as a function of $\tilde{\lambda}_U/\tilde{\lambda}_D$. A negative value of f_n/f_p is obtained in a narrow range of $\tilde{\lambda}_U/\tilde{\lambda}_D$ around -0.9 . The exact f_n/f_p value is very sensitive to the QCD corrections. The choice which gives maximal suppression for Xe as well as maximal relative scaling between Xe and Si is $f_n/f_p \simeq -0.7$, which occurs at $\tilde{\lambda}_U/\tilde{\lambda}_D \simeq -0.89$ and -0.92 when the QCD NLO correction is included or not, respectively ¹.

The key ingredient in achieving $\tilde{\lambda}_U/\tilde{\lambda}_D \sim -0.9$ is that the Higgs mediators have appropriately different couplings to up and down quarks. A 2HDM of Type II is such a model. Using Eq. (2.2) and the Higgs-quark couplings C_U, C_D of Table 1, a given value of f_n/f_p requires:

$$\tan \beta = - \frac{(f_n/f_p) F_u^p - (m_n/m_p) F_u^n}{(f_n/f_p) F_d^p - (m_n/m_p) F_d^n} \frac{w + \tan \alpha}{1 - w \tan \alpha} \quad (2.6)$$

¹The possible role of NLO/multi-particle interactions in determining the precise f_n/f_p value needed to minimize Xenon dark-matter scattering rate is discussed in [13].

Table 1. Tree-level vector boson couplings C_V ($V = W, Z$) and fermionic couplings C_F ($F = U, D$) normalized to their SM values for the Type II 2HDMs.

Higgs	C_V	C_U	C_D
h	$\sin(\beta - \alpha)$	$\cos \alpha / \sin \beta$	$-\sin \alpha / \cos \beta$
H	$\cos(\beta - \alpha)$	$\sin \alpha / \sin \beta$	$\cos \alpha / \cos \beta$
A	0	$\cot \beta$	$\tan \beta$

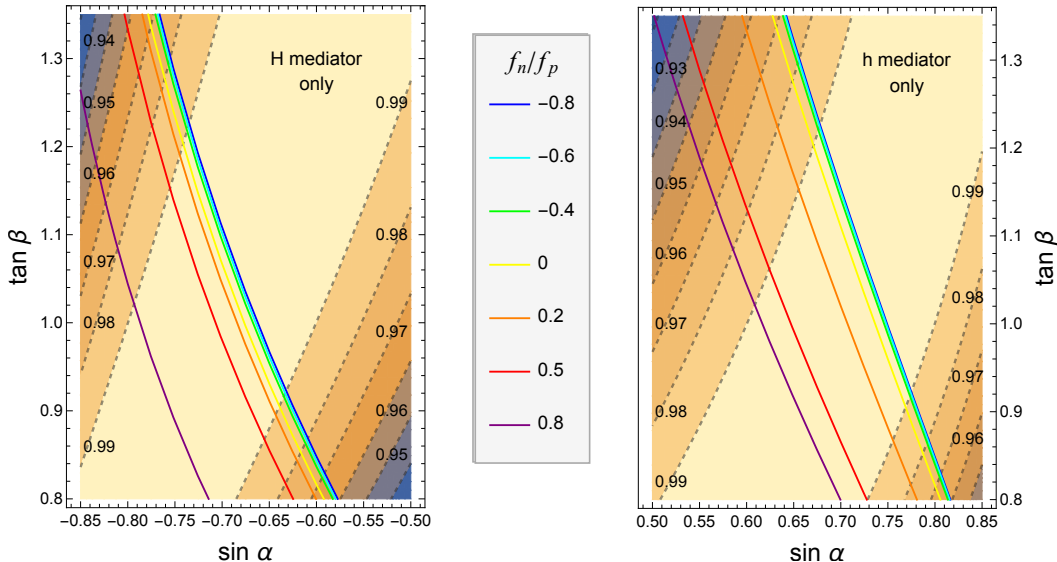


Figure 2. The left and right panels show contour plots (solid lines) of constant f_n/f_p in the $(\tan \beta, \sin \alpha)$ space for the case $m_h \sim 125$ GeV (H is the mediator) and $m_H \sim 125$ GeV (h is the mediator), respectively. NLO QCD corrections are taken into account. The dashed lines are contours of constant $\sin(\beta - \alpha)$ and $\cos(\beta - \alpha)$ in left and right panels, respectively.

where $w = \frac{\Lambda_h}{\Lambda_H} \frac{m_H^2}{m_h^2}$. Requiring that the SM-like Higgs has zero coupling to a pair of DM particles so as to avoid its having invisible decays, implies $w \rightarrow 0$ ($w \rightarrow \infty$) for the $h125$ ($H125$) scenario. In Fig. 2, we plot $\tan \beta$ versus $\sin \alpha$ in these two cases for various values of f_n/f_p . The value of $f_n/f_p \sim -0.7$ needed to suppress Xe limits corresponds to the very narrow band between the solid blue and cyan lines. In the figures, we also show (dashed) lines of constant $C_V^h = \sin(\beta - \alpha)$ ($C_V^H = \cos(\beta - \alpha)$) in the left (right) panels. Requiring $C_V^h \sim 1$ ($C_V^H \sim 1$) for the $h125$ ($H125$) to be very SM-like implies that $\tan \beta$ and $\sin \alpha$ must lie within the broad central yellow band. Combining this with the $f_n/f_p \sim -0.7$ requirement leaves only a small region in each of the $(\tan \beta, \sin \alpha)$ parameter spaces, located near $\tan \beta \sim 1$ and $\sin \alpha \sim -0.7$ ($+0.7$), implying $C_D^H \sim -C_U^H \sim 1$ ($C_U^h \sim -C_D^h \sim 1$) for the $h125$ ($H125$) scenario.

3 The 2HDMS Dark-Matter Model

Let us now consider the 2HDMS model in which a singlet scalar Higgs, S , is added to the 2HDM. The \mathbb{Z}'_2 symmetric and gauge-invariant 2HDMS scalar potential

was given in [15] and [6]. In the end, the terms associated with the S in the potential of importance to this study are:

$$V_S = \frac{m_S^2}{2} S^2 + v(\lambda_h h + \lambda_H H) S^2 + \lambda_{H^+H^-} H^+ H^- S^2 + \frac{\lambda_S}{4!} S^4 + (\lambda_{hh} hh + \lambda_{hH} hH + \lambda_{HH} HH + \lambda_{AAAA} AAAA) S^2. \quad (3.1)$$

(The previously employed generic portal couplings appearing in Eq. (2.5) are given by $\Lambda_{h,H} = -2\lambda_{h,H}$.)

Because its interactions are invariant under $S \rightarrow -S$, the S can be DM provided it does not acquire a vev. Further, the S does not affect the fits of [16, 17] to the LHC Higgs data so long as the 2HDM state of mass 125 GeV has small branching ratio to SS pairs. To avoid such decays we require $\lambda_h = 0$ or $\lambda_H = 0$ in the $h125$ or $H125$ scenarios, respectively. For our numerical work, we employ the $m_h = 125$ GeV or $m_H = 125$ GeV parameter points of [16, 17] that described the LHC Higgs data at the (rather stringent) 68% CL, supplemented by the latest $b \rightarrow s\gamma$ constraint of $m_{H^\pm} \gtrsim 480$ GeV for the Type II model [18]. For each such point, we scan over the independent singlet-sector parameters (m_S and λ_H or λ_h , respectively, fixing $\lambda_S = 2\pi$) and accept only points that satisfy perturbativity, tree level vacuum stability, tree level unitarity and for which a proper electroweak vacuum is achieved. We also require that the precision electroweak S and T parameters fall within $\pm 3\sigma$ of their observed values.

Dark matter relic abundance, $\Omega_S h^2$, is determined by the total DM annihilation rate. The relevant processes depend upon whether we consider the $h125$ or $H125$ scenario. For the $h125$ scenario, the amplitude diagrams for light dark matter ($m_S \leq 50$ GeV) are $SS \rightarrow H \rightarrow f\bar{f}$, $SS \rightarrow H \rightarrow \gamma\gamma$, and (relevant for $m_A \lesssim m_S$) $SS \rightarrow H \rightarrow AA$ and $SS \rightarrow AA$ via contact interaction. In the $H125$ scenario the SS annihilation tree-level diagrams are $SS \rightarrow h \rightarrow f\bar{f}$, $SS \rightarrow h \rightarrow \gamma\gamma$, $SS \rightarrow h \rightarrow hh$, $SS \rightarrow hh$ via t, u -channel S exchange and via contact interaction. ($SS \rightarrow AA$ annihilation does not occur since $m_A > 420$ GeV and the hh final states do not contribute unless $m_S \geq m_h$.) Also note that the parameter constraints needed to avoid large $\text{BR}(h \rightarrow AA)$ ($\text{BR}(H \rightarrow hh)$) when $m_A < m_h/2$ ($m_h < m_H/2$) in the $h125$ ($H125$) scenarios were studied in [17] and are incorporated in our 2HDM fits — they cause some variations of the phenomenology with m_A (m_h). For example, in the $h125$ case if $m_A < m_h/2$ then correct $\Omega_S h^2$ cannot be obtained if $m_A \geq m_S$, whereas if $m_A > m_h/2$ then $m_A > m_S$ for the range of m_S we consider and correct $\Omega_S h^2$ is easily obtained. Finally, we note that in the $H125$ case if $m_h \sim 2m_S$ then s-channel h exchange processes are strongly enhanced due to a resonance effect, whereas in the $h125$ case $m_H \sim 2m_S$ is not possible.

Thus, the main free parameter that determines $\Omega_S h^2$ in the $h125$ ($H125$) scenarios is λ_H (λ_h). As studied in [6], for any 2HDM parameter point accepted by the analysis of [16, 17] it is straightforward to find singlet-sector parameter choices for which the observed relic density lies within the $\pm 3\sigma$ window, $\Omega_S h^2 = 0.1187 \pm 0.0017$, after satisfying all the theoretical and experimental constraints related to the Higgs sector. (This is in sharp contrast to the xSM model mentioned in the Introduction.) In the figures to follow, only points that have $\Omega_S h^2$ in the above band (“correct” $\Omega_S h^2$) are shown.

3.1 Collider bounds from direct searches for Higgs bosons

Having taken into account the theoretical constraints on the 2HDMS and found parameter space points such that the S state in this model constitutes dark matter producing the entire thermal relic abundance, we now turn to bounds from searching for non-SM Higgs at the LHC. First of all, the available bounds for Higgs masses below 62.5 GeV were fully implemented in [17]. Since we employ the points from that paper in the present work, these bounds are automatically taken into account. In this section we shall discuss additional collider bounds that must be imposed coming from searches for light Higgs bosons in the mass range of 62.5 – 125 GeV at the LHC.

Possibly relevant direct Higgs production searches are: i) CMS [19] and ATLAS [20] limits on a light Higgs with mass $\gtrsim 90$ GeV decaying to $\tau\tau$ produced via gluon fusion or via $b\bar{b}$ associated production; and ii) CMS [21] limits on a light pseudoscalar Higgs boson of mass 25 – 80 GeV produced in association with $b\bar{b}$ and decaying to a pair of τ leptons.² We find that these two constraints do not eliminate any of our points due to the fact that the predicted cross sections are about 1-3 orders in magnitude below the experimental limits.

Next, we examine the consistency of our model points with the recent CMS result [22] on the search for a new heavy resonance decaying to a Z boson and a light resonance (h in our case), followed by $Z \rightarrow \ell\ell$ and the light resonance decaying to $b\bar{b}$ or $\tau\tau$. In our model, these limits apply to the process $A \rightarrow Zh \rightarrow \ell\ell h$ with $h \rightarrow b\bar{b}$ or $\tau\tau$. Unfortunately, since the experimental limits are given using overlapping color coding, it is not possible to use the experimental plots to get precise limits as a function of m_h and m_A . However, it is possible to extract the weakest and the strongest upper bounds at any given (m_h, m_A) . For $m_h < 62.5$ GeV, we find that the strongest (weakest) bound in the $b\bar{b}$ final state is 30 fb (100 fb) with corresponding bounds of 10 fb (100 fb) in the $\tau\tau$ final state. For $m_h > 62.5$ GeV, the strongest (weakest) bound in the $b\bar{b}$ final state is 10 fb (30 fb) with corresponding bounds of 3 fb (10 fb) in the $\tau\tau$ final state. It is convenient to compare these bounds to our model predictions by dividing the bound by the cross section for $gg \rightarrow A$ predicted in our model (taking $\tan\beta = 1$, as appropriate in our model). This gives us the “weak” and “strong” bounds on $\text{BR}(A \rightarrow Zh \rightarrow \ell\ell b\bar{b}/\tau\tau)$.

In Fig. 3, the points show our predicted $\text{BR}(A \rightarrow Zh \rightarrow \ell\ell b\bar{b}/\tau\tau)$ as a function of pseudoscalar mass m_A , with coloring according to the m_h value. The results are displayed separately for two different m_h ranges relevant for the subsequent discussion. In order to visualize the impact of the experimental data on our model, both the strong (minimal) and weak (maximal) upper limits on the cross section are shown by the black and gray curves in each plot, respectively. The points above the black (gray) curves would be excluded by the strong (weak) limits. We see that the strong upper limit in the $b\bar{b}$ final state removes many points with $m_h > 30$ GeV and thus significantly constrains the light Higgs h in the $H125$ scenario. In particular, for the case $m_h > 62.5$ GeV, this limit entirely eliminates the points in the bulk with $\text{BR}(h \rightarrow b\bar{b}) \geq 70\%$, pushing

²Direct computation reveals that the cross section for a light A and for a light h are very similar in magnitude in $b\bar{b}$ associated production (and gluon fusion). Thus, the limits of [21] are, in principle, relevant for $H125$ scenario in which there is a light h present.

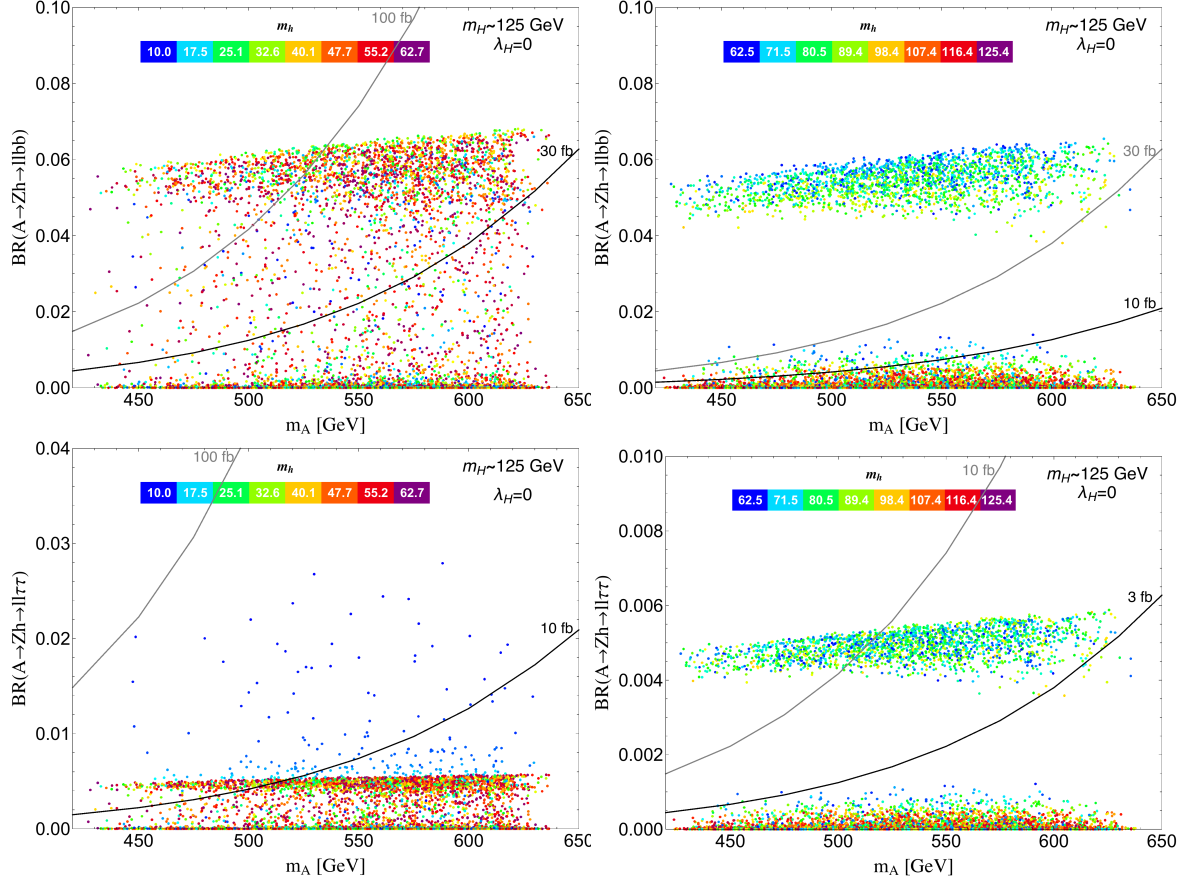


Figure 3. $\text{BR}(A \rightarrow Zh \rightarrow llbb)$ (upper) and $\text{BR}(A \rightarrow Zh \rightarrow ll\tau\tau)$ (lower) as a function of m_A . The point color indicates the value of m_h , which is below 62.5 GeV (left) and in the range of 62.5–125 GeV (right). We display the (strong and weak — see text) experimental upper limits on these branching ratios assuming A production via gluon-fusion, where for each point the branching ratio limit is computed by dividing the cross section limit by $\sigma(gg \rightarrow A)$ as computed taking $\tan\beta = 1$. In this scenario the heavy Higgs H is identified as the SM-like state at 125 GeV. All points shown can produce correct relic abundance and are not excluded by the LUX (2016) limit. Points below the black (gray) curve satisfy the strong (weak) constraints from non-SM-like Higgs searches at the LHC.

this branching ratio down to the 20% level. The $\tau\tau$ limits also have an impact for the $m_h \leq 30$ GeV points as shown in the lower left plot, while their importance becomes marginal below 15 GeV. For the purpose of showing the consistency of our model, we choose to adopt the ultra-conservative approach of imposing the strong upper limits — that is in subsequent plots and discussions we retain only the points below the black solid curves.

3.2 Collider bounds from jet plus missing energy final states

In this subsection, we consider the bounds from mono-jet+ \cancel{E}_T searches for dark matter. Such searches have been performed by the LHC experimental groups [23, 24],

although, to date, results from Run 2 are only available from ATLAS [25]. Unfortunately, they present their results under assumptions that do not apply to our model. Most critically, the effective operator approach is adopted to present the results. However, since the \cancel{E}_T cuts employed are of order 100's of GeV, the energy transfer in the collision exceeds the mediator (h) masses of interest to us and the effective operator approach is very inaccurate. In addition, our values of m_h are such that the h is mainly produced on-shell. Thus, we do not think that the bounds presented in the experimental papers can be applied to our analysis.

Generally speaking, constraints from mono-jet+ \cancel{E}_T searches will be applicable to our scenarios when properly analyzed. In our model, the h mediator is mainly produced on-shell and will yield \cancel{E}_T if the dark matter mass m_S is below $m_h/2$ and if $h \rightarrow SS$ decays are dominant, as is the case for many of our scan points (but not all). When the narrow width approximation is applicable, the jet+ \cancel{E}_T cross section is the same as for jet+ h times $\text{BR}(h \rightarrow SS)$. For the bulk of our points, $\text{BR}(h \rightarrow SS) \simeq 100\%$ implying little dependence of the cross section on the nature of DM. Further, if the \cancel{E}_T cuts are large, the implied jet energy will also be much larger than m_h and the jet+ h cross section will then depend weakly on m_h , rising only slowly as m_h decreases. For these reasons, the scalar-mediator results from the phenomenological analysis of [26] are applicable to our model despite the fact that they assume fermion dark matter and only consider mediator masses above 125 GeV. Their Figure 5 displays, as a function of m_h , the limit on the ratio, defined as μ , of the cross section for jet+ \cancel{E}_T relative to that predicted if the mediator couplings to SM fermions have SM values. In the narrow width approximation, this ratio is equal to the ratio of the mediator-coupling-squared to SM particles relative to SM strength. In their figure, only values of mediator mass, m_h , above 125 GeV are plotted, for which the limit is of order 2 – 4, falling slowly as m_h decreases. Extrapolation to lower m_h values suggests that it would only fall below 1 for m_h values below 20 – 30 GeV and maybe not even then. Since our h couplings are such that $\mu = 1$ is predicted, we conclude that the experimental limits from the 8 TeV, Run 1 data (and the projected limits from the 14 TeV, Run 2 data) do not exclude our preferred points.

Of course, many of our scan points have $m_h < 2m_S$, for which the mediator h decay is off-shell. While the mono-jet cross section in this case is more involved (proportional to the square of the product of the h couplings to DM and to SM fermions divided by the off-shell h propagator), the current constraints in this regime from the LHC turn out to be extremely weak [27].

3.3 Dark matter direct detection

In Fig. 4, we show the expected cross sections for S scattering off nuclei in Xenon-based detectors for both the $h125$ and $H125$ cases together with LUX (2016) results and the XENON1T future projection. The points are colored with respect to f_n/f_p . Note that, in accordance with expectations, points for which the cross section is suppressed correspond to f_n/f_p approaching -0.7 . The conclusion from the plots is that, after including isospin-violation, the 2HDMS could easily be consistent with both the LUX (2016) limits and also the limits anticipated for XENON1T. Conversely, future

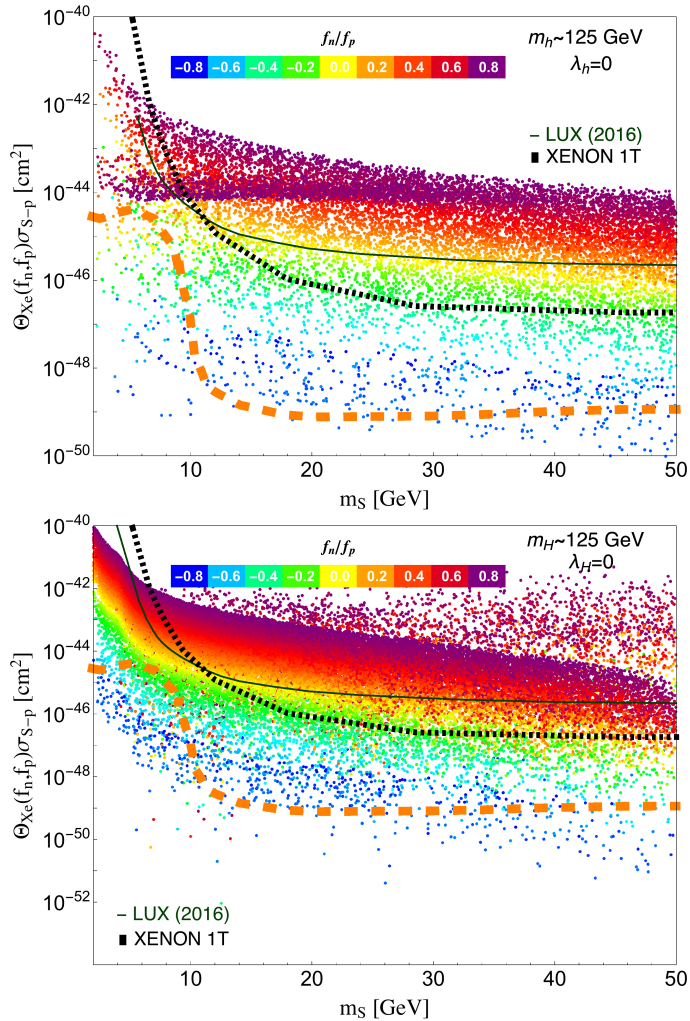


Figure 4. For points with correct $\Omega_S h^2$, we show $\Theta_{\text{Xe}}\sigma_{S-p}^{\text{SI}}$ vs. m_S for the h_{125} (upper) and H_{125} (lower) cases compared to the LUX (2016) bound [10] (solid dark green) and the XENON1T (2017) projections (dark dashed green boxes) [28]. All points shown satisfy the SuperCDMS limits. The neutrino coherent scattering dominates the recoil spectrum below the thick dashed orange line.

improved exclusion limits or positive signals will either place an upper bound on f_n/f_p or favor a particular value of f_n/f_p .

We have also examined the predicted cross sections for Si and Ge detectors. For both the h_{125} and H_{125} scenarios, our points (which satisfy the SuperCDMS and LUX (2016) limits) have cross sections at least two orders of magnitude below any of the tentative signals (CDMS-II [29, 30], DAMA [31], CoGeNT [32], and CRESST-II [33]) found in the low mass region.

3.4 Dark matter indirect detection

Finally, we consider the limits from indirect detection of SS annihilation products. If DM annihilates it could produce pairs of SM particles, such as electron-positron pairs

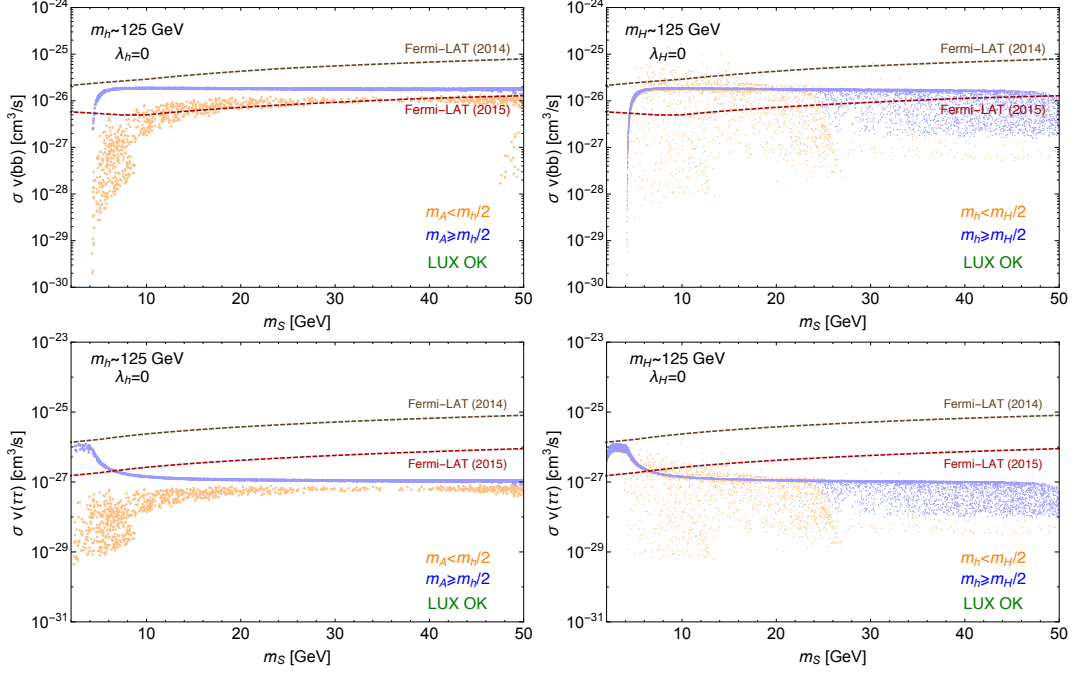


Figure 5. Indirect detection cross sections for $m_h \sim 125$ GeV (left) and $m_H \sim 125$ GeV (right) compared to Fermi-LAT limits for $b\bar{b}$ and $\tau^+\tau^-$ annihilations shown in the upper and lower panels, respectively. All points have correct $\Omega_S h^2$ and obey the LUX (2016) and SuperCDMS limits.

or photons. Currently, there are limits from the Fermi-LAT collaboration, see [34] and [35], on this annihilation cross section coming from the observation of the dwarf spheroidal galaxies of the Milky Way, which are the most DM-dominated objects we know of. We do not consider limits related to the observation of the Galactic Center [36] since they depend strongly on the choice of the DM profile.

Our results for indirect detection related to the $b\bar{b}$ and $\tau^+\tau^-$ final states are shown in Fig. 5. As described below, the $\tau^+\tau^-$ final state must be considered for $m_S \leq m_b$. In the $h125$ case, we observe that the points which survive the LUX (2016) limits and obey the Fermi-LAT (2015) limits are those with $m_A < 62.5$ GeV. Note that even a factor of 2 improvement in the Fermi-LAT limits would exclude all $h125$ points with $m_S \gtrsim 12$ GeV. In the $H125$ case, we compare points with $m_h < 62.5$ GeV to points with $m_h \geq 62.5$ GeV. Regardless of the m_h choice or the value of m_S , a large number of points survive the current Fermi-LAT limits and a significant fraction will also survive improved limits. In the $h125$ ($H125$) case, all the blue (all the) points shown below the $b\bar{b}$ threshold are eliminated by the $\tau^+\tau^-$ final state limits.

After all constraints, the LHC phenomenology of the non-SM-like 2HDM Higgs bosons is easily summarized. First, *all* must lie in definite mass ranges below 650 GeV. The allowed mass range for all scalar bosons in various scenarios is summarized in Table 2. Second, $\beta \sim \pi/4$ ($\tan \beta = 1$) and $\alpha \sim -\pi/4$ ($+\pi/4$) in the $h125$ ($H125$) Type II scenarios imply nearly unique Higgs-quark couplings. The resulting direct production cross sections at 13 TeV for all these non-SM-like 2HDM Higgs bosons will

Table 2. The allowed mass range for the scalars in various scenarios. The units are in GeV.

Scenario	m_S	m_h	m_H	m_A	m_{H^\pm}
$h125$	$\lesssim 12$	125	440 – 650	$\lesssim 62.5$	485 – 630
$H125$	$\gtrsim 4$	10 – 62.5	125	420 – 650	485 – 630
$H125$	$\gtrsim 25$	62.5 – 125	125	420 – 650	485 – 630

be substantial. Further, their decays will be such that detection should be possible. In the $h125$ scenario, $H^\pm \rightarrow tb$ is always dominant ($H^\pm \rightarrow HW^\pm$ is kinematically forbidden) while $H \rightarrow SS, AZ, t\bar{t}$ constitute the main decays for the H . In the relevant range of $m_A \lesssim 62.5$ GeV, $A \rightarrow b\bar{b}$ ($\tau\tau$) dominates for $m_A > 2m_b$ ($m_A < 2m_b$). For the $H125$ scenario, the important modes are $H^\pm \rightarrow hW^\pm, tb$ and $A \rightarrow Zh, t\bar{t}$. The h will decay to a mixture of $b\bar{b}$ and SS (invisible) final states. As an example, Ref. [37] claims that $t\bar{t}A$ production with $A \rightarrow b\bar{b}$ will be detectable at the LHC Run 2 for $\tan\beta = 1$ if $m_A \in [20, 100]$ GeV.

4 Conclusions

In a multi-Higgs model in which one Higgs fits the LHC 125 GeV state, one or more of the other Higgs bosons can mediate DM-nucleon interactions. We have shown that for appropriate Higgs-quark couplings maximal DM isospin violation is possible independent of the nature of DM. We then considered the explicit example of a Type II 2HDM where the h (H) is identified with the LHC 125 GeV state while the H (h) mediates the coupling between quarks and DM. This allows us to have DM of correct relic density that can even be maximally isospin violating (for 2HDM parameters $\tan\beta \sim 1$ and $\alpha \sim \pm\pi/4$), thereby evading LUX (2016) and future XENON1T limits even at low DM mass. If DM is discovered in the future, then the level of the observed direct detection cross section will determine the f_n/f_p value and the relevant $\tan\beta$ and α which can, hopefully, be checked against direct Higgs sector observations.

We next considered the 2HDMS model in which a scalar singlet, S , is added to the 2HDM, showing that it can be a viable DM particle in both the $h125$ and $H125$ scenarios. In the former (latter), the hSS (HSS) coupling can be sufficiently suppressed that the S does not affect the purely 2HDM fits of the h (H) to the 125 GeV signal, while the HSS (hSS) coupling can be chosen to give correct $\Omega_S h^2$. By employing appropriate isospin-violating 2HDM parameters, one can avoid direct and indirect detection limits even at low m_S . In this model, the non-SM-like Higgs bosons will be discovered during LHC Run 2 due to the fact that their masses and couplings are strongly restricted.

It is also worth mentioning that the single DM scalar scenario of the 2HDMS considered here can be easily extended to a multi-component DM sector with N real $O(N)$ -symmetric scalars in the spirit of [38].

Acknowledgments

JFG and YJ acknowledge partial support by US DOE grant DE-SC-000999. YJ also received generous support from LHC-TI fellowship US NSF grant PHY-0969510

and the Villum Foundation. He also acknowledges the LATPh for hospitality and particularly thanks Geneviève Bélanger for useful discussion and technical assistance regarding micrOMEGAs. The authors are also grateful to Yushin Tsai and Jian Wang for their helpful discussing the mono-jet search for dark matter at the LHC. The work of AD was supported by the STFC Grant ST/J002798/1. BG acknowledges partial support by the National Science Centre, Poland decision no DEC-2014/13/B/ST2/03969 and DEC-2014/15/B/ST2/00108. JFG acknowledges support during revision while at the Aspen Center for Physics, which is supported by National Science Foundation grant PHY-1066293.

References

- [1] **Planck** Collaboration, R. Adam et al., *Planck 2015 results. I. Overview of products and scientific results*, [arXiv:1502.01582](#).
- [2] D. S. Akerib et al., *Results from a search for dark matter in LUX with 332 live days of exposure*, [arXiv:1608.07648](#).
- [3] J. McDonald, *Gauge singlet scalars as cold dark matter*, Phys. Rev. **D50** (1994) 3637–3649, [[hep-ph/0702143](#)].
- [4] C. P. Burgess, M. Pospelov, and T. ter Veldhuis, *The Minimal model of nonbaryonic dark matter: A Singlet scalar*, Nucl. Phys. **B619** (2001) 709–728, [[hep-ph/0011335](#)].
- [5] X.-G. He, B. Ren, and J. Tandean, *Hints of Standard Model Higgs Boson at the LHC and Light Dark Matter Searches*, Phys. Rev. **D85** (2012) 093019, [[arXiv:1112.6364](#)].
- [6] A. Drozd, B. Grzadkowski, J. F. Gunion, and Y. Jiang, *Extending two-Higgs-doublet models by a singlet scalar field - the Case for Dark Matter*, JHEP **1411** (2014) 105, [[arXiv:1408.2106](#)].
- [7] X.-G. He and J. Tandean, *Low-Mass Dark-Matter Hint from CDMS II, Higgs Boson at the LHC, and Darkon Models*, Phys.Rev. **D88** (2013) 013020, [[arXiv:1304.6058](#)].
- [8] Y. Cai and T. Li, *Singlet Dark Matter in Type II Two Higgs Doublet Model*, Phys.Rev. **D88** (2013) 115004, [[arXiv:1308.5346](#)].
- [9] L. Wang and X.-F. Han, *A simplified 2HDM with a scalar dark matter and the galactic center gamma-ray excess*, Phys. Lett. **B739** (2014) 416–420, [[arXiv:1406.3598](#)].
- [10] **LUX Collaboration** Collaboration, D. Akerib et al., *First results from the LUX dark matter experiment at the Sanford Underground Research Facility*, Phys.Rev.Lett. **112** (2014) 091303, [[arXiv:1310.8214](#)].
- [11] **SuperCDMS** Collaboration, R. Agnese et al., *Search for Low-Mass Weakly Interacting Massive Particles with SuperCDMS*, Phys.Rev.Lett. **112** (2014), no. 24 241302, [[arXiv:1402.7137](#)].
- [12] J. L. Feng, J. Kumar, and D. Sanford, *Xenophobic Dark Matter*, Phys. Rev. **D88** (2013), no. 1 015021, [[arXiv:1306.2315](#)].
- [13] V. Cirigliano, M. L. Graesser, and G. Ovanesyan, *WIMP-nucleus scattering in chiral effective theory*, JHEP **10** (2012) 025, [[arXiv:1205.2695](#)].

- [14] G. Belanger, F. Boudjema, A. Pukhov, and A. Semenov, *micrOMEGAs-3: A program for calculating dark matter observables*, Comput. Phys. Commun. **185** (2014) 960–985, [[arXiv:1305.0237](#)].
- [15] B. Grzadkowski and P. Osland, *Tempered Two-Higgs-Doublet Model*, Phys.Rev. **D82** (2010) 125026, [[arXiv:0910.4068](#)].
- [16] B. Dumont, J. F. Gunion, Y. Jiang, and S. Kraml, *Constraints on and future prospects for Two-Higgs-Doublet Models in light of the LHC Higgs signal*, Phys. Rev. **D90** (2014) 035021, [[arXiv:1405.3584](#)].
- [17] J. Bernon, J. F. Gunion, Y. Jiang, and S. Kraml, *Light Higgs bosons in Two-Higgs-Doublet Models*, Phys. Rev. **D91** (2015), no. 7 075019, [[arXiv:1412.3385](#)].
- [18] M. Misiak et al., *Updated NNLO QCD predictions for the weak radiative B-meson decays*, Phys. Rev. Lett. **114** (2015), no. 22 221801, [[arXiv:1503.01789](#)].
- [19] **ATLAS** Collaboration, G. Aad et al., *Search for neutral Higgs bosons of the minimal supersymmetric standard model in pp collisions at $\sqrt{s} = 8$ TeV with the ATLAS detector*, JHEP **11** (2014) 056, [[arXiv:1409.6064](#)].
- [20] **CMS** Collaboration, V. Khachatryan et al., *Search for neutral MSSM Higgs bosons decaying to a pair of tau leptons in pp collisions*, JHEP **10** (2014) 160, [[arXiv:1408.3316](#)].
- [21] **CMS** Collaboration, V. Khachatryan et al., *Search for a low-mass pseudoscalar Higgs boson produced in association with a $b\bar{b}$ pair in pp collisions at $\sqrt{s} = 8$ TeV*, Phys. Lett. **B758** (2016) 296–320, [[arXiv:1511.03610](#)].
- [22] **CMS** Collaboration, V. Khachatryan et al., *Search for neutral resonances decaying into a Z boson and a pair of b jets or tau leptons*, Phys. Lett. **B759** (2016) 369–394, [[arXiv:1603.02991](#)].
- [23] **CMS** Collaboration, V. Khachatryan et al., *Search for dark matter, extra dimensions, and unparticles in monojet events in protonproton collisions at $\sqrt{s} = 8$ TeV*, Eur. Phys. J. **C75** (2015), no. 5 235, [[arXiv:1408.3583](#)].
- [24] **ATLAS** Collaboration, G. Aad et al., *Search for new phenomena in final states with an energetic jet and large missing transverse momentum in pp collisions at $\sqrt{s} = 8$ TeV with the ATLAS detector*, Eur. Phys. J. **C75** (2015), no. 7 299, [[arXiv:1502.01518](#)]. [Erratum: Eur. Phys. J. **C75**, no. 9, 408 (2015)].
- [25] **ATLAS** Collaboration, M. Aaboud et al., *Search for new phenomena in final states with an energetic jet and large missing transverse momentum in pp collisions at $\sqrt{s} = 13$ TeV using the ATLAS detector*, Phys. Rev. **D94** (2016), no. 3 032005, [[arXiv:1604.07773](#)].
- [26] P. Harris, V. V. Khoze, M. Spannowsky, and C. Williams, *Constraining Dark Sectors at Colliders: Beyond the Effective Theory Approach*, Phys. Rev. **D91** (2015) 055009, [[arXiv:1411.0535](#)].
- [27] J. Abdallah et al., *Simplified Models for Dark Matter and Missing Energy Searches at the LHC*, [arXiv:1409.2893](#).
- [28] **XENON1T** Collaboration, E. Aprile, *The XENON1T Dark Matter Search Experiment*, Springer Proc. Phys. **148** (2013) 93–96, [[arXiv:1206.6288](#)].

- [29] **CDMS Collaboration** Collaboration, R. Agnese et al., *Silicon detector results from the first five-tower run of CDMS II*, Phys.Rev. **D88** (2013) 031104, [[arXiv:1304.3706](#)].
- [30] **CDMS Collaboration** Collaboration, R. Agnese et al., *Silicon Detector Dark Matter Results from the Final Exposure of CDMS II*, Phys.Rev.Lett. **111** (2013) 251301, [[arXiv:1304.4279](#)].
- [31] R. Bernabei, P. Belli, F. Cappella, V. Caracciolo, S. Castellano, et al., *Final model independent result of DAMA/LIBRA-phase1*, Eur.Phys.J. **C73** (2013) 2648, [[arXiv:1308.5109](#)].
- [32] **CoGeNT collaboration** Collaboration, C. Aalseth et al., *Results from a Search for Light-Mass Dark Matter with a P-type Point Contact Germanium Detector*, Phys.Rev.Lett. **106** (2011) 131301, [[arXiv:1002.4703](#)].
- [33] G. Angloher, M. Bauer, I. Bavykina, A. Bento, C. Bucci, et al., *Results from 730 kg days of the CRESST-II Dark Matter Search*, Eur.Phys.J. **C72** (2012) 1971, [[arXiv:1109.0702](#)].
- [34] **Fermi-LAT** Collaboration, M. Ackermann et al., *Dark matter constraints from observations of 25 Milky Way satellite galaxies with the Fermi Large Area Telescope*, Phys.Rev. **D89** (2014) 042001, [[arXiv:1310.0828](#)].
- [35] **Fermi-LAT** Collaboration, M. Ackermann et al., *Searching for Dark Matter Annihilation from Milky Way Dwarf Spheroidal Galaxies with Six Years of Fermi-LAT Data*, [arXiv:1503.02641](#).
- [36] T. Daylan, D. P. Finkbeiner, D. Hooper, T. Linden, S. K. N. Portillo, N. L. Rodd, and T. R. Slatyer, *The Characterization of the Gamma-Ray Signal from the Central Milky Way: A Compelling Case for Annihilating Dark Matter*, [arXiv:1402.6703](#).
- [37] M. Casolino, T. Farooque, A. Juste, T. Liu, and M. Spannowsky, *Probing a light CP-odd scalar in di-top-associated production at the LHC*, Eur. Phys. J. **C75** (2015) 498, [[arXiv:1507.07004](#)].
- [38] A. Drozd, B. Grzadkowski, and J. Wudka, *Multi-Scalar-Singlet Extension of the Standard Model - the Case for Dark Matter and an Invisible Higgs Boson*, JHEP **1204** (2012) 006, [[arXiv:1112.2582](#)].